

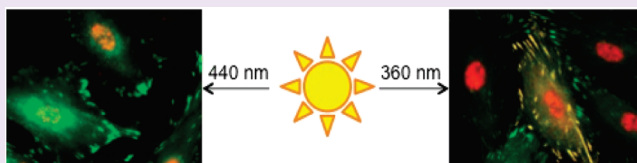
# Dual Wavelength Photoactivation of cAMP- and cGMP-Dependent Protein Kinase Signaling Pathways

Melanie A. Priestman, Liang Sun, and David S. Lawrence\*

Department of Chemistry, the Division of Medicinal Chemistry & Natural Products, School of Pharmacy, and the Department of Pharmacology, School of Medicine, The University of North Carolina at Chapel Hill, Chapel Hill, North Carolina 27599, United States

**S** Supporting Information

**ABSTRACT:** The spatial and temporal organization of biological systems offers a level of complexity that is challenging to probe with conventional reagents. Photoactivatable (caged) compounds represent one strategy by which spatiotemporal organizational complexities can be addressed. However, since the vast majority of caged species are triggered by UV light, it is not feasible to *orthogonally* control two or more spatiotemporal elements of the phenomenon under investigation. For example, the cGMP- and cAMP-dependent protein kinases are highly homologous enzymes, separated in time and space, which mediate the phosphorylation of both distinct and common protein substrates. However, current technology is unable to discriminate, in a temporally or spatially selective fashion, between these enzymes and/or the pathways they influence. We describe herein the intracellular triggering of a cGMP-mediated pathway with 360 nm light and the corresponding cAMP-mediated pathway with 440 nm light. Dual wavelength photoactivation was assessed in A10 cells by monitoring the phosphorylation of vasodilator-stimulated phosphoprotein (VASP), a known substrate for both the cAMP- and cGMP-dependent protein kinases. Illumination at 440 nm elicits a cAMP-dependent phosphorylation of VASP at Ser157, whereas 360 nm exposure triggers the phosphorylation of both Ser157 and Ser239. This is the first example of wavelength-distinct activation of two separate nodes of a common signaling pathway.



Biological behavior is inherently dynamic, be it at the cellular, tissue, organ, or organismal level.<sup>1</sup> The response of living organisms and their component parts to environmental stimuli often reflects the spatiotemporal elements associated with that stimulus. For example, metastasis is driven by the directed migration of tumor cells toward spatially focused chemoattractant gradients.<sup>2</sup> However, spatiotemporal control of biological behavior is not limited to just environmental stimuli. As a result of evolution's efficiency, individual proteins and the biochemical pathways they inhabit are often used for more than one purpose. The activation of a specific protein can have a multitude of biological consequences yet, within the appropriate spatiotemporal context, elicit only a single response. Cytochrome *c*, as a key member of the mitochondrial electron transport chain, is essential for life in eukaryotes. However, upon release from the mitochondrion, it serves as a purveyor of death.<sup>3</sup> Only a micrometer separates life from death, a fact that highlights the control exerted by the spatiotemporal context under which the biological event occurs. Unfortunately, conventional probes of cellular biochemistry, such as inhibitors, activators, or sensors, typically lack the temporal or spatial resolution to adequately address biochemically driven behaviors, especially those that transpire during a short time frame or occur within a restricted spatial environment.

A wide variety of photoactivatable (caged) compounds and biomolecules have been described since their first introduction in the late 1970s.<sup>4–9</sup> These species are biologically inactive until exposed to high intensity light, most commonly at the UV–vis boundary ( $\sim 360$  nm).<sup>7–15</sup> This special property allows bioactive

species to be loaded into a biological system *in an inert form*. Subsequent exposure to light, delivered as a high photon flux with a sharp focus, can furnish a degree of spatiotemporal control not feasible through conventional means. However, a number of challenges remain before this technology can be utilized to address some of the pressing issues that lie at the frontiers of biological research. For example, the degree of spatial resolution is constrained by both the diffraction limit of light as well as by the rapid diffusion of caged and photoactivated molecules into and out of the illuminated region of interest. In addition, the investigator is typically forced to take, as an article of faith, that uncaging has been successful. These issues have recently been addressed by attaching caged compounds to localization sequences (spatial control)<sup>16</sup> and by linking the photoactivation process to a fluorescence increase (confirmation of uncaging).<sup>16–18</sup> Perhaps most challenging, however, is the complexity of signaling pathways and the limited impact that a single agent may have in helping to elucidate the dynamic properties associated with these intracellular processes. A potentially powerful advance would be the ability to selectively activate two or more bioreagents, thereby providing separate spatiotemporal control at two or more nodes (*e.g.*, activation and inhibition) of a signaling pathway.

We describe herein the use of wavelength-distinguishable photolabile moieties to create triggers for two closely related

**Received:** December 6, 2010

**Accepted:** January 11, 2011

**Published:** January 11, 2011

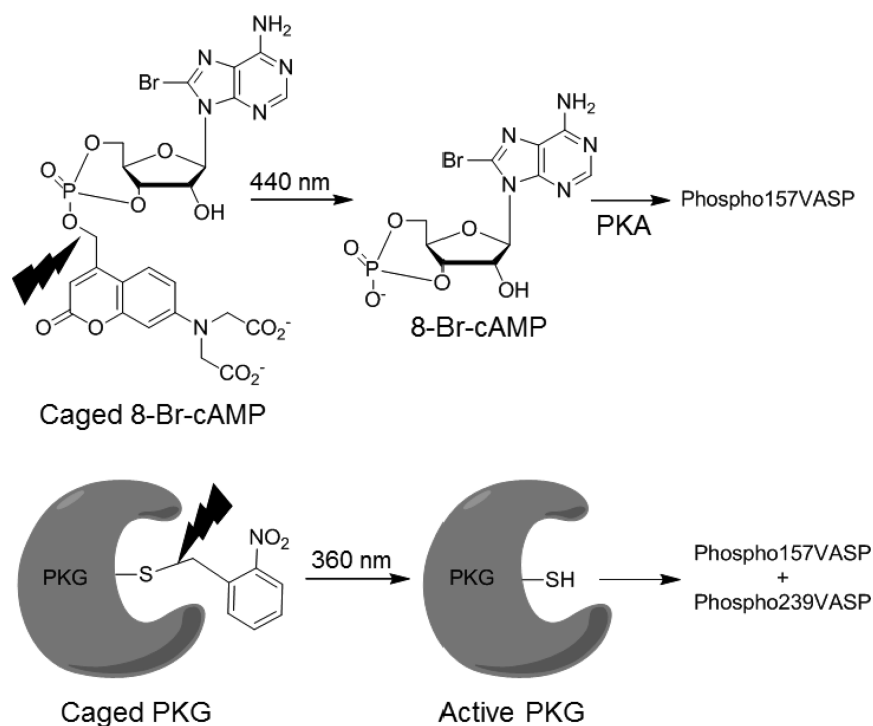


**Figure 1.** Dual wavelength photoactivation of PKA and PKG pathways. (Top) Coumarin-caged cAMP is photolyzed with 440 nm light, resulting in the activation of PKA and subsequent phosphorylation of VASP at Ser157. (Bottom) Nitrobenzyl-caged PKG is photolyzed with 360 nm light, resulting in phosphorylation of VASP at Ser157 and Ser239.

signaling pathways, namely, those mediated by the cAMP- and cGMP-dependent protein kinases (PKA and PKG, respectively) (Figure 1). PKA and PKG possess 70% sequence homology in their catalytic domains<sup>19</sup> and exhibit the same consensus sequence preferences with respect to peptide-based substrates. However, their downstream effects range from overlapping to distinct.<sup>20–22</sup> For example, both enzymes have been implicated in cell motility through their direct action on vasodilator-stimulated phosphoprotein (VASP), a member of the Ena/VASP family of proteins.<sup>23</sup> VASP is regulated by phosphorylation at Ser157, Ser239, and Thr278, which promotes changes in protein–protein interactions of the actin network.<sup>23</sup> The latter interactions, in turn, regulate cell motility.<sup>24</sup> However, the PKA- and PKG-mediated phosphorylation of VASP, particularly in cells, is the subject of considerable controversy.<sup>23,25–28</sup> Although it has been reported that PKA acts preferentially at Ser157, and PKG at Ser239,<sup>29</sup> the kinetics of phosphorylation appears to be a function of many factors including levels of cyclic nucleotides, the intracellular concentration of PKA and PKG, and cell type.<sup>23,25–28</sup> A potentially confounding issue is that pathway activation is dependent upon a myriad of inputs and/or is subject to deactivation by endogenous regulatory mechanisms. We've addressed these issues in the context of wavelength-selective triggering of PKA and PKG action on VASP. First, since the activation of these pathways can be initiated by cyclic nucleotides or by enzymes themselves, we've explored both possibilities by generating a light activatable cyclic nucleotide and using it in combination with a light-triggerable protein kinase. Second, we've bypassed the assortment of intracellular regulatory mechanisms by using caged species that, upon photolysis, are constitutively activated and thus resistant to up- or down-regulation by endogenous enzymes or other factors. These strategies furnish the means to trigger, in a wavelength-selective fashion, the cAMP- and cGMP-dependent protein kinase pathways.

## RESULTS AND DISCUSSION

There is overwhelming evidence that signaling pathways and the cellular behavior that they mediate are profoundly influenced by the spatial and/or temporal context in which they operate. Indeed, cells exhibit a remarkable ability to process two or more spatiotemporal inputs and subsequently render a decision concerning the behavioral course of action.<sup>1</sup> Unfortunately, conventional reagents are limited in their ability to probe pathway performance with a high degree of spatial or temporal resolution, particularly with respect to multiple inputs. One attractive strategy is the use of two or more photosensitive reagents that can be activated with light in a selective fashion. This may be achieved with reagents that are distinguished by pronounced differences in their photolytic quantum yields, in their sensitivity to two-photon (versus conventional) photolysis, or on the basis of their wavelength sensitivity. For any given pair of reagents, a minimum requirement is simply that one of the two reagents is activatable without disturbing the other. Indeed, Ellis-Davies and his colleagues recently employed two-photon illumination to discriminate between a dinitroindolyl caged glutamate and that of an aminocoumarin-caged  $\gamma$ -aminobutyric acid.<sup>30</sup> Desired receptor activation was achieved *via* the proper control of laser power, light wavelength, and caged compound concentrations. An alternative strategy, namely, the use of photolysis wavelength alone to distinguish between differentially caged species, enjoys the potential advantage of ready application across a broad biological platform such as subcellular-, cellular-, and multi-cellular-based settings, including analyses that range from single cells (*e.g.*, microscopy) to large cell populations (*e.g.*, Western blot and flow cytometry readouts). In addition, a variety of sources can be used to deliver light of desired wavelengths to the sample, from relatively inexpensive systems (Hg or Xe lamps

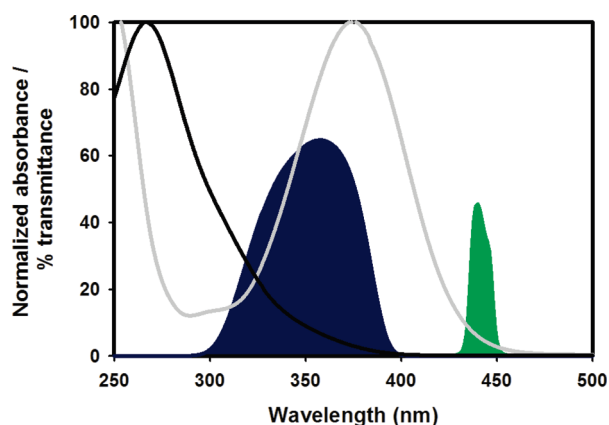


**Figure 2.** UV scans of nitrobenzyl bromide (black) and the coumarin (gray) caging groups overlaid with the transmittance of the UV (blue) and 440 nm (green) bandpass filters. Absorbance of nitrobenzyl bromide and coumarin caging units was normalized setting the major peak at 100.

coupled with appropriate filters) to higher end lasers. The photolabile nitrobenzyl moiety (near UV), in conjunction with far UV<sup>31–33</sup> or visible light-sensitive caging groups,<sup>34–38</sup> has paved the way for wavelength-selective photoactivatable pairs, such as protecting groups recently reported for thiols.<sup>38</sup> We employed the latter to create wavelength-selective triggers for the highly homologous PKA and PKG pathways.

**Selection of Photosensitive Moieties.** Dual wavelength photoactivation of multiple biological molecules requires the use of photosensitive groups that can be cleaved at separate wavelengths. For this reason the *o*-nitrobenzyl moiety was employed in combination with an amino-substituted coumarin derivative<sup>36,37</sup> to cage PKG and 8-Br-cAMP, respectively (Figure 1). The coumarin absorbs at wavelengths longer than 450 nm, whereas the nitrobenzyl moiety displays no significant absorbance beyond 400 nm (Figure 2). A “white light” source (Hg arc lamp) was employed, in combination with a 440 ± 10 nm bandpass filter, to selectively photolyze the coumarin-caged cAMP (*vide infra*). By contrast, a UV bandpass filter (300–390 nm window that is centered at 360 nm) was used to activate the nitrobenzyl-caged PKG (Figure 2 and *vide infra*).

**Caged cGMP-Independent PKG.** The caged reagents developed in this study are endowed with the following key property: upon photoactivation, the active species is impervious to either up- or down-regulation by intracellular processes. Specifically, we employed a cAMP derivative that is not prone to inactivation by phosphodiesterase-mediated hydrolysis. Furthermore, we constructed a PKG mutant that is not dependent upon cGMP for activity. Consequently, in both cases, the corresponding caged analogues, upon photolysis, produce species that are instantaneously active and remain so throughout the duration of the experiment.

Single site-directed mutagenesis was carried out using a baculovirus expression vector to generate a constitutively active, cGMP-independent, Ile63Ser PKG.<sup>39</sup> This mutation was confirmed by sequence analysis. The mutant enzyme was expressed in Sf9 insect cells using a baculoviral expression system as previously described.<sup>40</sup> The PKG mutant was purified on a 8-(2-aminoethyl)aminoadenosine-3',5'-cyclic monophosphate (8-AEA-cAMP) agarose resin with typical yields of 2–3 mg per liter of harvested Sf9 cells, at greater than 95% purity (Supplemental

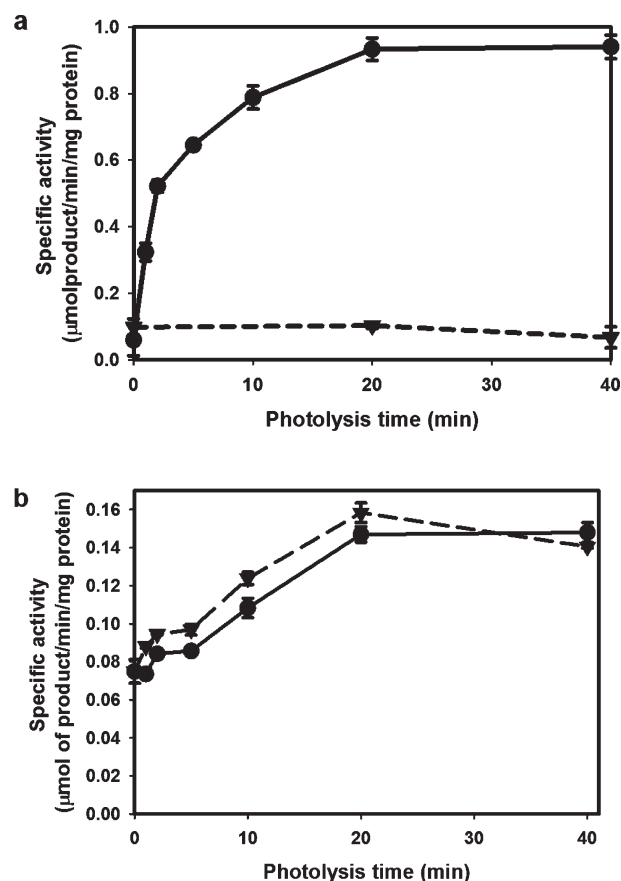


**Figure 3.** Photoactivation of nitrobenzyl-caged PKG and coumarin-caged 8-Br-cAMP. (a) Fold increase in specific activity of caged PKG due to photolysis using either the 360 nm bandpass filter (solid, ●) or the 440 nm bandpass filter (dashed, ▼). (b) Fold increase in specific activity of PKA holoenzyme due to photoactivation of caged 8-Br-cAMP with either the 360 nm bandpass filter (solid, ●) or the 440 nm bandpass filter (dashed, ▼). Data are represented as averages with standard errors of three independent assays.

Figure 1). Activation of wild-type and Ile63Ser PKG was assessed in the absence and presence of cGMP, thereby confirming that the mutant enzyme is constitutively active (specific activity of  $1.44 \pm 0.05 \mu\text{mol}/\text{min}/\text{mg}$  without and  $1.53 \pm 0.04 \mu\text{mol}/\text{min}/\text{mg}$  with cGMP) but that wild-type PKG activity is dependent on cGMP ( $0.16 \pm 0.02 \mu\text{mol}/\text{min}/\text{mg}$  without and  $1.00 \pm 0.10 \mu\text{mol}/\text{min}/\text{mg}$  with cGMP) (Supplemental Figure 2).

Preparation of a caged Ile63Ser PKG required modification of one or more residues at or near the active site so that catalytic activity is compromised. Previous studies have revealed that modification of Cys518 inactivates PKG.<sup>41</sup> Therefore, we employed a thiol reactive reagent to generate a caged PKG whose activity can be restored by 360 nm photolysis (Figure 3a). We do note that PKG contains 11 cysteine residues per monomer, of which eight are accessible without denaturation.<sup>42</sup> Ellman's titration revealed that nitrobenzylbromide modifies 5–6 cysteine residues on Ile63SerPKG (Supplemental Figure 3). Restoration of PKG activity is in proportion to illumination time (Figure 3a and Supplemental Figure 4a), thereby confirming that the process is light dependent. Complete activation requires 20 min of photolysis. This relatively long time frame is a consequence of the experimental setup, namely, benchtop photolysis of a macroscopic sample contained within an eppendorf tube.

By contrast, photolysis under a microscope transpires through a narrow beam that delivers an intense photon flux to a highly focused region (e.g., a single cell), resulting in photolysis times shorter than 1 s.<sup>14</sup> Caged Ile63Ser PKG displays a specific activity of  $0.06 \pm 0.05 \mu\text{mol}/\text{min}/\text{mg}$ , which is 4.6% of the activity displayed by Ile63Ser PKG, and 360 nm photolysis of the caged enzyme generates a 15.7-fold increase of enzymatic activity ( $0.94 \pm 0.04 \mu\text{mol}/\text{min}/\text{mg}$ ). By contrast, no increase in enzymatic activity was observed upon exposure of the caged enzyme to 440 nm light. The relative activity values (15.7-fold) displayed by pre- and postphotolyzed caged PKG compare favorably to those of unstimulated and cGMP-stimulated wild-type PKG (i.e., 6- to 10-fold).<sup>43</sup> Photoactivation of caged PKG was examined at a variety of wavelengths (Supplemental Figure 5). As expected, regeneration of PKG activity is most efficient at 360 nm, presumably due to the large overlap with the absorbance spectrum of the nitrobenzyl moiety. Nevertheless, there is significant activation of the caged enzyme at 400 nm, 405 and 410 nm. Although photolysis of the nitrobenzyl moiety likely proceeds with a low quantum yield at these wavelengths,<sup>44</sup> the intense H-line emission (405 nm) of the Hg arc lamp light source may be responsible for the photocleavage observed in the 400–410 nm range. However, illumination at 420 or 440 nm (Hg G line) fails to activate caged PKG.

**Caged 8-Substituted cAMP.** 8-Substituted-cAMP derivatives are hydrolyzed very slowly by phosphodiesterases relative to cAMP itself.<sup>45</sup> Consequently, we utilized a caged derivative of 8-Br-cAMP so that, upon photolysis, a comparatively long-lived active analogue of cAMP is unleashed. The 7-[bis(carboxymethyl)amino]coumarin derivative of 8-Br-cAMP was prepared as previously reported.<sup>36,37</sup> The PKA holoenzyme ( $0.08 \pm 0.01 \mu\text{mol}/\text{min}/\text{mg}$ ) displays a 2-fold increase ( $0.16 \pm 0.02 \mu\text{mol}/\text{min}/\text{mg}$ ) in activity upon exposure to 8-Br-cAMP (10  $\mu\text{M}$ ). All commercially available sources of PKA holoenzyme tested have a high level of residual activity, and all display a similar modest response to cAMP. The coumarin-caged 8-Br-cAMP was unable to stimulate PKA holoenzyme ( $0.08 \pm 0.01 \mu\text{mol}/\text{min}/\text{mg}$ ) until photolyzed at either 360 nm ( $0.15 \pm 0.01 \mu\text{mol}/\text{min}/\text{mg}$ ) or at 440 nm ( $0.16 \pm 0.01 \mu\text{mol}/\text{min}/\text{mg}$ ) (Figure 3b and Supplemental Figure 4b).

**PKA- and PKG-Mediated Phosphorylation of VASP.** PKA and PKG regulate VASP activity by phosphorylating residues Ser157 and Ser239, but the pattern and kinetics of phosphorylation by these two enzymes remains controversial.<sup>23,25–28</sup> We investigated the selectivity of PKA- and PKG-catalyzed phosphorylation at these two sites in A10 cells. Cells were serum starved and then stimulated with either 100  $\mu\text{M}$  8-Br-cAMP or 8-Br-cGMP. VASP phosphorylation was monitored by Western blot (lysates) and by immunofluorescence (fixed cells) using pSer157-selective and pSer239-selective antibodies. VASP is only phosphorylated at Ser157 by cAMP stimulation but both Ser157 and Ser239 are phosphorylated when the cells are stimulated with cGMP (Supplemental Figures 6a and 7a–c). Lysates from serum starved cells were also incubated with increasing concentrations of constitutively active PKA or PKG (Supplemental Figure 6b). The phosphorylation pattern is similar to that observed with the cyclic nucleotide treated cells, namely, PKA fails to phosphorylate Ser239 except at very high concentrations (5.3  $\mu\text{M}$ ) and PKG phosphorylates both residues even at the lowest concentration tested (26 nM). The distinct VASP phosphorylation patterns induced by these cyclic nucleotide-dependent protein kinases furnished the means to monitor wavelength-selective activation of PKA and PKG.

**Light-Triggered VASP Phosphorylation with Caged Analogues of cAMP and PKG.** A10 cells were loaded with the long wavelength (440 nm) caged analogue of cell-permeable 8-Br-cAMP and the short wavelength (360 nm) caged derivative of PKG, which was microinjected. VASP phosphorylation was monitored in the absence and presence of photolysis (360 or 440 nm). VASP phosphorylation at Ser157 and Ser239 was observed in cells containing caged PKG, but only upon illumination at 360 nm (Figure 4a–c). Microinjection of mouse IgG, caged PKG in the absence of photolysis, or caged PKG exposed to 440 nm all fail to induce VASP phosphorylation. Illumination of noninjected cells at 360 or 440 nm likewise has no effect on phosphorylation status. It should be noted that in all phospho-Ser157 VASP immunofluorescence experiments there appears to be low levels of phosphorylation even prior to stimulation. This is a consequence of the antibody used in these experiments, which appears to display some affinity for nonphosphorylated VASP as assessed by Western blot analysis (data not shown). In addition, the total fluorescence reading for each experiment varied as a result of storage of the antibody over time. Consequently, 8-Br-cAMP and 8-Br-cGMP were always run as controls for all experiments. We note as an aside that the released photolyzed caging byproducts (in particular the potentially electrophilic *o*-nitrosobenzaldehyde) do not appear to have deleterious consequences in terms of VASP phosphorylation. These results are consistent with the general absence of observed harmful consequences of these species on cellular integrity.<sup>46</sup>

Cell-permeable caged 8-Br-cAMP was simply incubated with A10 cells for 30 min at 37 °C prior to photolysis at either 360 or 440 nm. Both photolytic conditions induce phosphorylation of the PKA-specific site Ser157 (Figure 5a–c). This selective phosphorylation is consistent with the results observed with 8-Br-cAMP stimulation. In the absence of photolysis, however, caged 8-Br-cAMP fails to trigger VASP phosphorylation, demonstrating that intracellular PKA was not activated. Finally, dual wavelength photoactivation of PKA and PKG signaling pathways in A10 cells was carried out by loading cells with both the long wavelength sensitive caged 8-Br-cAMP and the UV sensitive caged PKG. Photolysis at 440 nm furnishes selective activation of the PKA pathway, namely, phosphorylation of VASP at Ser157, whereas both the PKA and PKG pathways are activated at 360 nm, as demonstrated by the phosphorylation of Ser157 and Ser239 (Figure 6a–c).

The caged reagents employed in this study were designed with several features in mind. First, these species, upon photoactivation, are constitutively active and thus impervious to potentially interfering up- or down-regulation by the endogenous biochemistry of the cell. A previously described cGMP-independent PKG mutant<sup>39</sup> and the phosphodiesterase-resistant 8-Br-cAMP<sup>45</sup> were used as the biochemical triggers to activate the PKG and PKA pathways, respectively. Second, selective photolysis was achieved by employing two photosensitive moieties, only one of which is removed by wavelengths greater than 420 nm. Specifically, the nitrobenzyl-caged PKG is only photolyzed at wavelengths shorter than 410 nm, whereas the coumarin-caged cyclic nucleotide is sensitive to wavelengths up to and including 440 nm. Third, caged enzymes, upon photolysis, enjoy “specificity of action” but lack cell permeability, whereas caged small molecules (e.g., cAMP) can be rendered cell-permeable but often display off-target effects. We chose one example from each category to demonstrate the utility of wavelength-selective perturbation of cell signaling. Fourth, photolysis was achieved using a white light

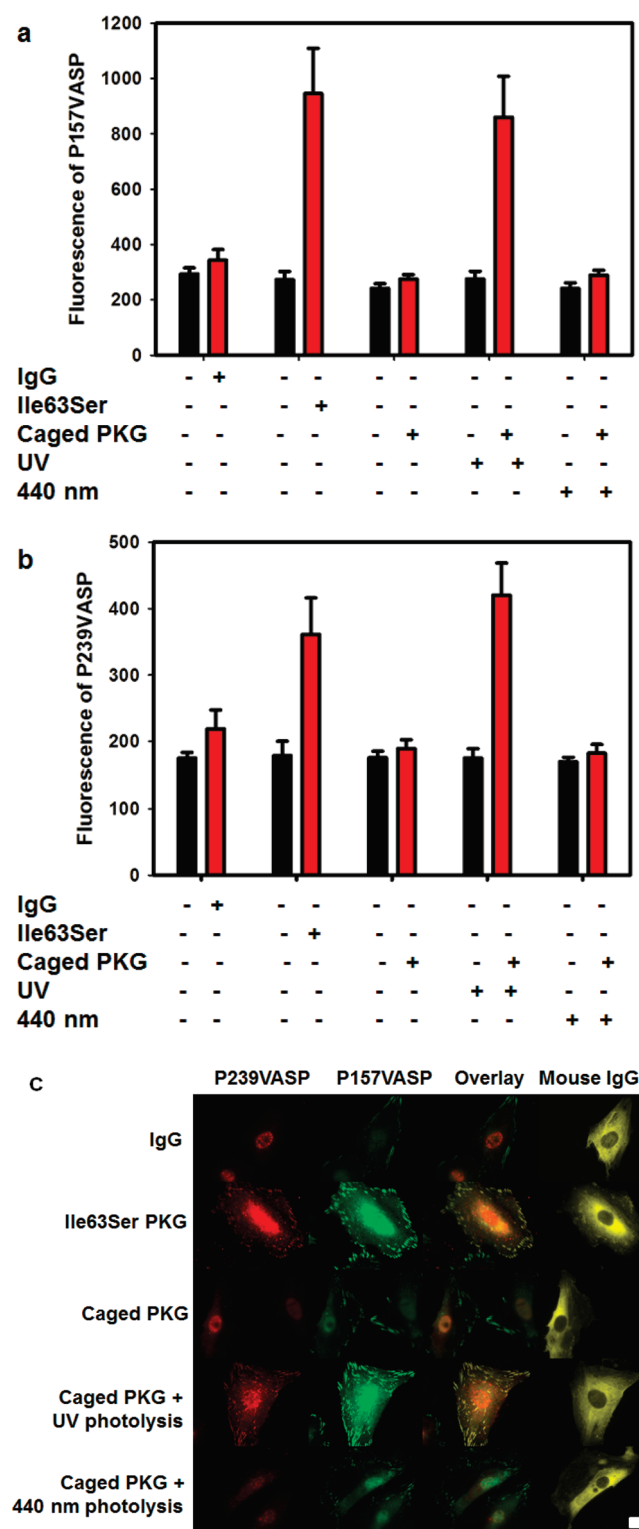


**Figure 4.** Photoactivation of nitrobenzyl-caged PKG leads to phosphorylation of Ser157 and Ser239 on VASP in A10 cells. Quantification of the immunofluorescence of phospho157VASP (a) and phospho239VASP (b) in A10 cells microinjected with caged PKG. (c) Immunofluorescent images of A10 cells microinjected with caged PKG. A10 cells were either stimulated with 100  $\mu$ M 8-Br-cGMP or microinjected with 50  $\mu$ M caged PKG. Data are represented as averages of 5–25 cells with standard errors. Scale bar is 40  $\mu$ m.

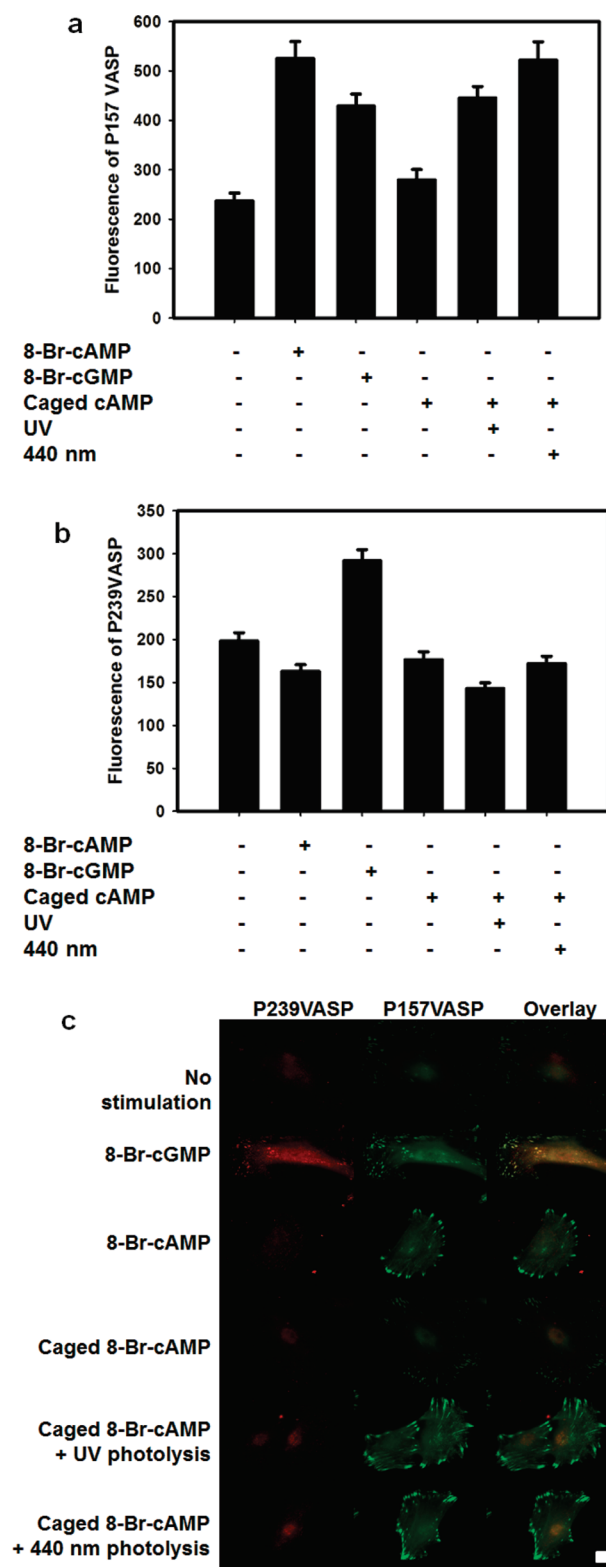


**Figure 5.** Photoactivation of coumarin-caged 8-Br-cAMP leads to phosphorylation of Ser157 and Ser239 on VASP in A10 cells. Quantification of the immunofluorescence of phospho157VASP (a) and phospho239VASP (b) in A10 cells loaded with caged 8-Br-cAMP. (c) Immunofluorescent images of A10 cells loaded with caged 8-Br-cAMP. A10 cells were either stimulated with 100  $\mu$ M 8-Br-cAMP, 100  $\mu$ M 8-Br-cGMP or loaded with 100  $\mu$ M caged 8-Br-cAMP. Data are represented as averages of 5–25 cells with standard errors. Scale bar is 40  $\mu$ m.

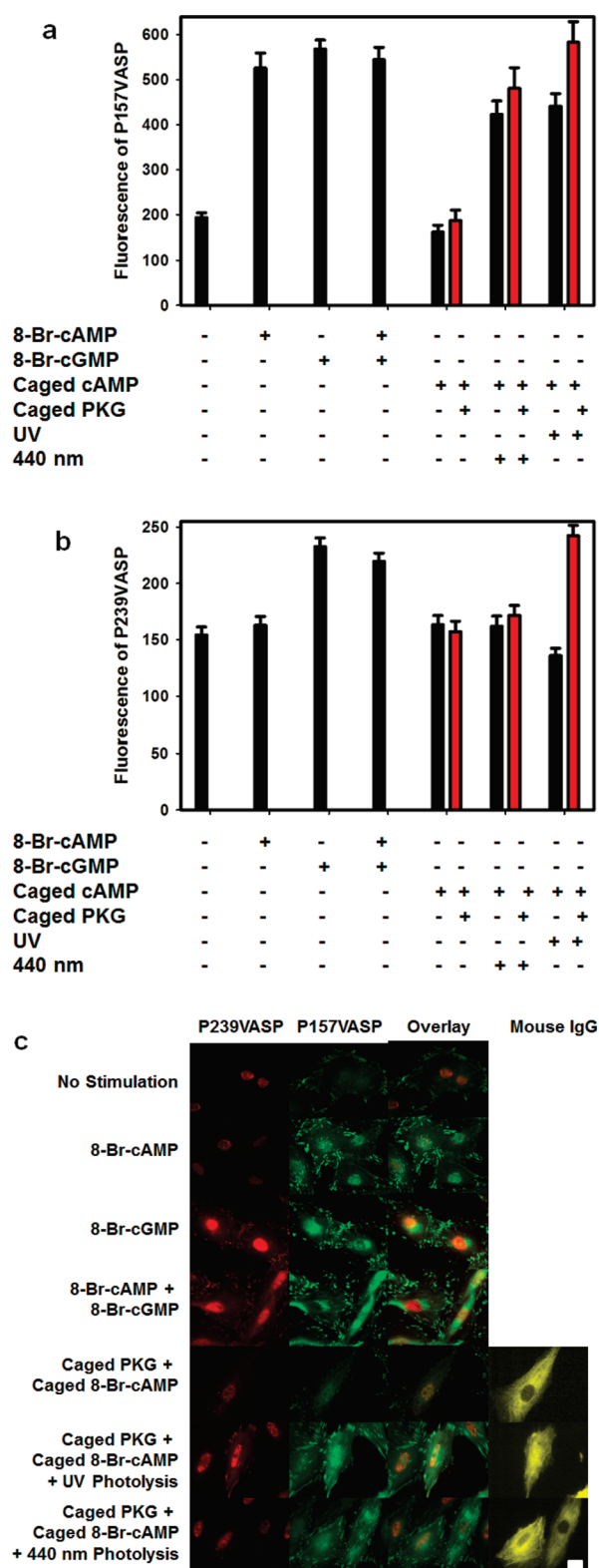


**Figure 6.** Wavelength-selective triggering of PKA and PKG in A10 cells. Quantification of (a) phospho157VASP and (b) phospho239VASP via immunofluorescence in A10 cells loaded with caged 8-Br-cAMP and/or microinjected with caged PKG. (c) Images of A10 cells loaded with caged 8-Br-cAMP and/or microinjected with caged PKG. A10 cells were either stimulated with 100  $\mu$ M 8-Br-cAMP, 100  $\mu$ M 8-Br-cGMP, loaded with 100  $\mu$ M caged 8-Br-cAMP, and/or microinjected with 50  $\mu$ M caged PKG. Data are represented as averages of 5–25 cells with standard errors.

source in conjunction with edge or band filters, all of which are inexpensive and commercially available. Finally, we note that both the coumarin and nitrobenzyl moieties absorb and suffer photolysis at 360 nm. Consequently, orthogonal activation of two separate phenomena requires that long wavelength (440 nm) light serves as the initial trigger and short wavelength (360 nm) as the concluding trigger. However, the coumarin and nitrobenzyl moieties can be interchangeably used as caging moieties on bioactive species, thereby providing the investigator with the triggering sequence option of his or her choice.

## METHODS

**Materials.** 2-Nitrobenzyl bromide, 8-Br-cAMP, 8-Br-cGMP, and PKA holoenzyme were purchased from Sigma. GST tagged PKGI $\alpha$  was purchased from Invitrogen. All primary antibodies and HRP secondary antibodies were from Santa Cruz Technologies. Secondary antibodies used for immunofluorescence were from Invitrogen. Cell culture media and solutions were from Invitrogen. Competent DH5 $\alpha$  cells were from Stratagene, Sf9 insect cells were from Invitrogen, and A10 cells were from the tissue culture facility at the University of North Carolina. All other chemicals were from Fisher or Sigma unless otherwise noted.

**Assessment of PKG and PKA Activity.** The *in vitro* activities of PKG and the PKA holoenzyme were determined using a coupled enzyme assay and either Leu-Arg-Arg-Arg-Arg-Phe-Ser-amide or Leu-Arg-Arg-Ala-Ser-Leu-Gly substrates, both of which were synthesized by standard Fmoc solid phase peptide synthesis.<sup>47</sup> Briefly, phosphorylation of the peptide was coupled to pyruvate kinase and lactate dehydrogenase resulting in the oxidation of NADH. Formation of the latter was monitored at 340 nm. Pyruvate kinase and lactate dehydrogenase were maintained as nonrate limiting enzymes. The activities of PKG and PKA were determined in 50 mM Tris pH 7.5, 100 mM NaCl, 10 mM MgCl<sub>2</sub>, 10% glycerol, 1 mM peptide, 1 mM ATP, 1 mM DTT, 1 mM phosphoenol pyruvate, and 0.2 mM NADH  $\pm$  10  $\mu$ M 8-Br-cAMP or 8-Br-cGMP.

**Preparation of Caged Ile63Ser PKG.** Ile63Ser PKG was extensively dialyzed against 50 mM Tris pH 7.5, 100 mM NaCl, 10 mM MgCl<sub>2</sub>, and 10% glycerol to remove all trace amounts of reducing reagents prior to modification with nitrobenzyl bromide. The latter was conducted with 6  $\mu$ M Ile63Ser PKG and 1 mM nitrobenzyl bromide maintained at 4  $^{\circ}$ C for 4 days. The reaction was quenched with 10 mM DTT and then dialyzed against buffer to remove the nitrobenzyl-DTT adduct.

**Photolysis.** Photolysis was carried out using an Oriel 200 W Hg arc lamp (model 68700) equipped with a beam bending filter. A UV bandpass colored glass filter (Newport, FSQ-UG1), 400 nm  $\pm$  10 nm bandpass filter (Newport, 10BPF10-400), 405 nm  $\pm$  10 nm bandpass filter (Newport, 10BPF10-405), 410 nm  $\pm$  10 nm bandpass filter (Newport, 10BPF10-410), 420 nm  $\pm$  10 nm bandpass filter (Newport, 10BPF10-420) and a 440 nm  $\pm$  10 nm bandpass filter (Newport, 10BPF10-440) were used for wavelength-selective photolysis. For *in vitro* assays, caged-PKG or caged-cAMP were photolyzed in an eppendorf tube and irradiated for up to 40 min on ice and then added to the coupled assay. A10 cells were photolyzed using the same filters in MatTek gridded glass bottom dishes for 15 min and then allowed to recover for 1 h at 37  $^{\circ}$ C with 5% CO<sub>2</sub>.

**Microscopy.** All fluorescent microscopy imaging was performed with an inverted Olympus IX81 microscope equipped with a Hamamatsu C8484 camera, 60X oil immersion Plan S-Apo objective and FITC, TxRed, and Cy5.5 filter cubes (Semrock). Microinjection was conducted with an Eppendorf FemtoJet and Injectman NI 2 system attached to the microscope set at 100 hPa injection pressure for 0.7 s. Metamorph or Image J software were employed for imaging analysis and overlays.

**Cell Culture.** A10 rat aortic smooth muscle cells were passaged by treatment with 0.5% trypsin + 0.53 mM EDTA before reaching confluence and maintained in DMEM containing 20% fetal bovine

serum (FBS) supplemented with gentamycin and kanamycin at 37 °C in a 5% CO<sub>2</sub> incubator. Two days prior to microscopy experiments, cells were plated into either MatTek 6-well glass bottom dishes for cell-permeable studies or MatTek 50 mm gridded glass bottom dishes for microinjection studies. The day prior to the microscopy experiments, all cells were serum starved in DMEM containing 2% FBS with gentamycin and kanamycin at 37 °C in a 5% CO<sub>2</sub> incubator. On the day of the microscopy experiments, the media was replaced with Leibovitz's L-15 without phenol red supplemented with 2% FBS.

**Immunofluorescence.** Serum starved A10 cells were loaded with 100 μM coumarin 8-Br-cAMP for 30 min at 37 °C and then washed 3 times with L-15 media or were microinjected with 10 mg/mL purified mouse IgG (sigma) ± 50 μM PKG constructs. Photolysis of cells was carried out as described above and cells were allowed to recover for 1 h at 37 °C with 5% CO<sub>2</sub> before fixing. Noninjected control cells were stimulated with 100 μM 8-Br-cAMP and/or 8-Br-cGMP for 1 h prior to fixation. All cells were briefly washed with PBS and fixed with 4% paraformaldehyde (Electron Microscopy Sciences) for 15 min at RT. Cells were then washed with PBS, permeabilized with 0.5% triton on ice for 20 min, washed with PBS, and blocked with 5% donkey serum for 3 h. Fixed cells were incubated with 1:50 dilution of the primary antibodies in donkey serum overnight at 4 °C, washed, and incubated with 1:500 secondary antibodies in donkey serum at RT for 2 h. After incubation with antibodies, cells were washed with PBS and imaged on the microscope with the appropriate filters. Primary antibodies: (1) for controls, 1:125 normal goat IgG + 1:125 normal rabbit IgG as controls; (2) for phospho239 VASP and VASP staining, 1:50 goat anti-phospho239VASP + 1:50 rabbit anti-VASP; and (3) for phospho239VASP and phospho157VASP staining, 1:50 goat anti-phospho239VASP + 1:50 rabbit anti-phospho157VASP. Secondary antibodies: (1) for studies with cell-permeable reagents, 1:500 donkey anti-goat Alexa 568 + 1:500 donkey anti-rabbit Alexa 488 and (2) for microinjection studies, 1:500 donkey anti-goat Alexa 568 + 1:500 donkey anti-rabbit Alexa 488 + 1:500 donkey anti-mouse Alexa 680.

## ■ ASSOCIATED CONTENT

**Supporting Information.** This material is available free of charge via the Internet at <http://pubs.acs.org>.

## ■ AUTHOR INFORMATION

### Corresponding Author

\*Fax: 919-962-2388. E-mail: [lawrencd@email.unc.edu](mailto:lawrencd@email.unc.edu).

## ■ ACKNOWLEDGMENT

Postdoctoral support for M.A.P. from NIH training grant 5T32 HL07675-18 at the Albert Einstein College of Medicine. The National Institutes of Health (RO1-CA079954) is gratefully acknowledged for generous financial support.

## ■ REFERENCES

- (1) Kholodenko, B. N., Hancock, J. F., and Kolch, W. (2010) Signalling ballet in space and time. *Nat. Rev. Mol. Cell. Biol.* 11, 414–426.
- (2) Kedrin, D., van Rheenen, J., Hernandez, L., Condeelis, J., and Segall, J. E. (2007) Cell motility and cytoskeletal regulation in invasion and metastasis. *J. Mammary Gland Biol. Neoplasia* 12, 143–152.
- (3) Liu, X., Kim, C. N., Yang, J., Jemerson, R., and Wang, X. (1996) Induction of apoptotic program in cell-free extracts: requirement for dATP and cytochrome c. *Cell* 86, 147–157.
- (4) Engels, J., and Schlaeger, E. J. (1977) Synthesis, structure, and reactivity of adenosine cyclic 3',5'-phosphate benzyl triesters. *J. Med. Chem.* 20, 907–911.
- (5) Kaplan, J. H., Forbush, B., 3rd, and Hoffman, J. F. (1978) Rapid photolytic release of adenosine 5'-triphosphate from a protected analogue: utilization by the Na:K pump of human red blood cell ghosts. *Biochemistry* 17, 1929–1935.
- (6) Dorman, G., and Prestwich, G. D. (2000) Using photolabile ligands in drug discovery and development. *Trends Biotechnol.* 18, 64–77.
- (7) Goeldner, M., Givens, R. (2005) *Dynamic Studies in Biology: Phototriggers, Photoswitches and Caged Biomolecules*, Wiley-VCH, Weinheim.
- (8) Marriott, G., and Ottl, J. (1998) Synthesis and applications of heterobifunctional photocleavable cross-linking reagents. *Methods Enzymol.* 291, 155–175.
- (9) Mayer, G., and Heckel, A. (2006) Biologically active molecules with a "light switch". *Angew. Chem., Int. Ed.* 45, 4900–4921.
- (10) Adams, S. R., and Tsien, R. Y. (1993) Controlling cell chemistry with caged compounds. *Annu. Rev. Physiol.* 55, 755–784.
- (11) Pelliccioli, A. P., and Wirz, J. (2002) Photoremovable protecting groups: reaction mechanisms and applications. *Photochem. Photobiol. Sci.* 1, 441–458.
- (12) Conrad, P. G., 2nd, Givens, R. S., Weber, J. F., and Kandler, K. (2000) New phototriggers: extending the p-hydroxyphenacyl pi-pi absorption range. *Org. Lett.* 2, 1545–1547.
- (13) Dmochowski, I. J., and Tang, X. (2007) Taking control of gene expression with light-activated oligonucleotides. *Biotechniques* 43, 161, 163, 165 passim.
- (14) Lee, H. M., Larson, D. R., and Lawrence, D. S. (2009) Illuminating the chemistry of life: design, synthesis, and applications of "caged" and related photoresponsive compounds. *ACS Chem. Biol.* 4, 409–427.
- (15) Young, D. D., and Deiters, A. (2007) Photochemical control of biological processes. *Org. Biomol. Chem.* 5, 999–1005.
- (16) Lee, H. M., Priestman, M. A., and Lawrence, D. S. (2010) Light-mediated spatial control via photolabile fluorescently quenched peptide cassettes. *J. Am. Chem. Soc.* 132, 1446–1447.
- (17) Pellois, J. P., Hahn, M. E., and Muir, T. W. (2004) Simultaneous triggering of protein activity and fluorescence. *J. Am. Chem. Soc.* 126, 7170–7171.
- (18) Gagey, N., Neveu, P., Benbrahim, C., Goetz, B., Aujard, I., Baudin, J. B., and Jullien, L. (2007) Two-photon uncaging with fluorescence reporting: evaluation of the o-hydroxycinnamic platform. *J. Am. Chem. Soc.* 129, 9986–9998.
- (19) Takio, K., Wade, R. D., Smith, S. B., Krebs, E. G., Walsh, K. A., and Titani, K. (1984) Guanosine cyclic 3',5'-phosphate dependent protein kinase, a chimeric protein homologous with two separate protein families. *Biochemistry* 23, 4207–4218.
- (20) Abdel-Latif, A. A. (2001) Cross talk between cyclic nucleotides and polyphosphoinositide hydrolysis, protein kinases, and contraction in smooth muscle. *Exp. Biol. Med. (Maywood, NY, U.S.)* 226, 153–163.
- (21) Keef, K. D., Hume, J. R., and Zhong, J. (2001) Regulation of cardiac and smooth muscle Ca(2+) channels (Ca(V)1.2a,b) by protein kinases. *Am. J. Physiol. Cell Physiol.* 281, C1743–1756.
- (22) Lincoln, T. M., Dey, N., and Sellak, H. (2001) Invited review: cGMP-dependent protein kinase signaling mechanisms in smooth muscle: from the regulation of tone to gene expression. *J. Appl. Physiol.* 91, 1421–1430.
- (23) Krause, M., Dent, E. W., Bear, J. E., Loureiro, J. J., and Gertler, F. B. (2003) Ena/VASP proteins: regulators of the actin cytoskeleton and cell migration. *Annu. Rev. Cell Dev. Biol.* 19, 541–564.
- (24) Bear, J. E., Loureiro, J. J., Libova, I., Fassler, R., Wehland, J., and Gertler, F. B. (2000) Negative regulation of fibroblast motility by Ena/VASP proteins. *Cell* 101, 717–728.
- (25) Bear, J. E., and Gertler, F. B. (2009) Ena/VASP: towards resolving a pointed controversy at the barbed end. *J. Cell Sci.* 122, 1947–1953.
- (26) Burkhardt, M., Glazova, M., Gambaryan, S., Vollkommer, T., Butt, E., Bader, B., Heermeier, K., Lincoln, T. M., Walter, U., and Palmethofer, A. (2000) KTS823 inhibits cGMP-dependent protein

kinase activity in vitro but not in intact human platelets and rat mesangial cells. *J. Biol. Chem.* 275, 33536–33541.

(27) Howe, A. K., Hogan, B. P., and Juliano, R. L. (2002) Regulation of vasodilator-stimulated phosphoprotein phosphorylation and interaction with Abl by protein kinase A and cell adhesion. *J. Biol. Chem.* 277, 38121–38126.

(28) Lindsay, S. L., Ramsey, S., Aitchison, M., Renne, T., and Evans, T. J. (2007) Modulation of lamellipodial structure and dynamics by NO-dependent phosphorylation of VASP Ser239. *J. Cell Sci.* 120, 3011–3021.

(29) Benz, P. M., Blume, C., Seifert, S., Wilhelm, S., Waschke, J., Schuh, K., Gertler, F., Munzel, T., and Renne, T. (2009) Differential VASP phosphorylation controls remodeling of the actin cytoskeleton. *J. Cell Sci.* 122, 3954–3965.

(30) Kantevari, S., Matsuzaki, M., Kanemoto, Y., Kasai, H., and Ellis-Davies, G. C. (2010) Two-color, two-photon uncaging of glutamate and GABA. *Nat. Methods* 7, 123–125.

(31) Blanc, A., and Bochet, C. G. (2002) Wavelength-controlled orthogonal photolysis of protecting groups. *J. Org. Chem.* 67, 5567–5577.

(32) Bochet, C. G. (2001) Orthogonal Photolysis of Protecting Groups. *Angew. Chem., Int. Ed. Engl.* 40, 2071–2073.

(33) Pirrung, M. C., Fallon, L., Zhu, J., and Lee, Y. R. (2001) Photochemically removable silyl protecting groups. *J. Am. Chem. Soc.* 123, 3638–3643.

(34) Furuta, T., Wang, S. S., Dantzker, J. L., Dore, T. M., Bybee, W. J., Callaway, E. M., Denk, W., and Tsien, R. Y. (1999) Brominated 7-hydroxycoumarin-4-ylmethyls: photolabile protecting groups with biologically useful cross-sections for two photon photolysis. *Proc. Natl. Acad. Sci. U.S.A.* 96, 1193–1200.

(35) Hagen, V., Frings, S., Wiesner, B., Helm, S., Kaupp, U. B., and Bendig, J. (2003) [7-(Dialkylamino)coumarin-4-yl]methyl-caged compounds as ultrafast and effective long-wavelength phototriggers of 8-bromo-substituted cyclic nucleotides. *ChemBioChem* 4, 434–442.

(36) Hagen, V., Bendig, J., Frings, S., Eckardt, T., Helm, S., Reuter, D., and Kaupp, U. B. (2001) Highly efficient and ultrafast phototriggers for cAMP and cGMP by using long-wavelength UV/vis-activation. *Angew. Chem., Int. Ed.* 40, 1045–1048.

(37) Hagen, V., Dekowski, B., Nache, V., Schmidt, R., Geissler, D., Lorenz, D., Eichhorst, J., Keller, S., Kaneko, H., Benndorf, K., and Wiesner, B. (2005) Coumarinylmethyl esters for ultrafast release of high concentrations of cyclic nucleotides upon one- and two-photon photolysis. *Angew. Chem., Int. Ed.* 44, 7887–7891.

(38) Kotzur, N., Briand, B., Beyermann, M., and Hagen, V. (2009) Wavelength-selective photoactivatable protecting groups for thiols. *J. Am. Chem. Soc.* 131, 16927–16931.

(39) Yuasa, K., Michibata, H., Omori, K., and Yanaka, N. (2000) Identification of a conserved residue responsible for the autoinhibition of cGMP-dependent protein kinase Ialpha and beta. *FEBS Lett.* 466, 175–178.

(40) Feil, R., Muller, S., and Hofmann, F. (1993) High-level expression of functional cGMP-dependent protein kinase using the baculovirus system. *FEBS Lett.* 336, 163–167.

(41) Puri, R. N., Bhatnagar, D., Glass, D. B., and Roskoski, R., Jr. (1985) Inactivation of guanosine cyclic 3',5'-monophosphate dependent protein kinase from bovine lung by o-phthalaldehyde. *Biochemistry* 24, 6508–6514.

(42) Landgraf, W., Regulla, S., Meyer, H. E., and Hofmann, F. (1991) Oxidation of cysteines activates cGMP-dependent protein kinase. *J. Biol. Chem.* 266, 16305–16311.

(43) Busch, J. L., Bessay, E. P., Francis, S. H., and Corbin, J. D. (2002) A conserved serine juxtaposed to the pseudosubstrate site of type I cGMP-dependent protein kinase contributes strongly to autoinhibition and lower cGMP affinity. *J. Biol. Chem.* 277, 34048–34054.

(44) Aujard, I., Benbrahim, C., Gouget, M., Ruel, O., Baudin, J. B., Neveu, P., and Jullien, L. (2006) o-nitrobenzyl photolabile protecting groups with red-shifted absorption: syntheses and uncaging cross-sections for one- and two-photon excitation. *Chemistry* 12, 6865–6879.

(45) Michal, G., Muhlegger, K., Nelboeck, M., Thiessen, C., and Weimann, G. (1974) Cyclophosphates VI. Cyclophosphates as substrates and effectors of phosphodiesterase. *Pharmacol Res Commun* 6, 203–252.

(46) Mitchison, T. J. (1989) Polewards microtubule flux in the mitotic spindle: evidence from photoactivation of fluorescence. *J. Cell Biol.* 109, 637–652.

(47) Wood, J. S., Yan, X., Mendelow, M., Corbin, J. D., Francis, S. H., and Lawrence, D. S. (1996) Precision substrate targeting of protein kinases. The cGMP- and cAMP-dependent protein kinases. *J. Biol. Chem.* 271, 174–179.